Full Paper Transactions, SMiRT 28
Toronto, Canada, August 10-15, 2025

INFLUENCE OF THERMAL GRADIENTS ON THE STRUCTURAL RESPONSE OF A CONTAINMENT STRUCTURE DURING LEAKAGE-RATE TESTING ACROSS DIFFERENT SEASONS

Marcelo A. Ceballos[1], Federico Pinto[2], Carlos F. Estrada[3], Antonio M. Prato[4], Carlos A. Prato[5]

[1]Professor, FCEFyN Univ. Nac. de Córdoba – IDIT CONICET, Córdoba (marcelo.ceballos@unc.edu.ar)
[2]Professor, FCEFyN Universidad Nacional de Córdoba – IDIT CONICET, Córdoba (fpinto@unc.edu.ar)
[3]Professor, FCEFyN Universidad Nacional de Córdoba, Córdoba (carlos.estrada@unc.edu.ar)
[4]Professor, FCEFyN Universidad Nacional de Córdoba, Córdoba (antprato@yahoo.com)
[5]Emeritus Professor, FCEFyN Universidad Nacional de Córdoba, Córdoba (prato_carlos@yahoo.com)

ABSTRACT

The Containment Structure of a Nuclear Power Plant (NPP) with over 40 years of service is periodically subjected to leak-tightness tests as part of a maintenance program This paper describes the results of the mechanical behavior analysis during the last two tests conducted in 2018 and 2024 at different times of the year. The objective of this evaluation is to detect any structural anomalies in relation to the expected response, which is obtained through a numerical model of the structure. The response measurement is performed using displacement transducers placed on the inner surface of the Containment Structure. These measurements are significantly affected by daily thermal variations, which occur particularly on the outer surface during the pressurization phase, lasting approximately one week. This observation has already been extensively documented in other publications on similar leak-tightness tests. The strategy used to filter out temperature variations consists of subtracting the thermally induced displacements, calculated with the numerical model, from the total measured displacements. For this approach to be effective, the model must accurately represent the temperature distribution across the thickness of the structural elements as an initial condition for the simulation. A particular aspect analyzed is the deformation of the base slab caused by pressure, which induces an almost rigid-body rotation of the Internal Structure—where the transducers are mounted—distorting the displacement measurements.

INTRODUCTION

A nuclear power plant in the province of Córdoba, Argentina, was subjected to two leakage rate tests: one in the summer of 2018 (Ceballos et al., 2019; Pinto et al., 2024) and another in late winter/early spring of 2024. The thermal gradients during these tests differed due to seasonal variations. Structural displacements caused by internal pressures were significantly influenced by temperature changes, as the tests spanned several days. This paper compares the influence of thermal gradients on structural response in both cases, highlighting the critical need to incorporate these effects into the structural model. Proper modeling ensures accurate assessment of behavior under applied pressures while filtering out displacements induced by thermal variations. Kim et al. (2018) and Wang et al. (2019) emphasize the impact of thermal fluctuations on structural behavior during pressure tests, while Cheng et al. (2022) conduct a similar study. Unlike those works, which focus primarily on strains, this study emphasizes displacements, as their experimental measurements are less affected by local conditions.

One notable observation of the latest campaign is that the displacements measured along a meridian of the cylindrical wall of the Containment Structure are greater than those predicted by the model, while on the diametrically opposite meridian, the measured displacements are consistently smaller. According to predictions made using the same model, this discrepancy may be attributed to the deformation of the base

slab, which supports both the Containment Structure (CS) and the Internal Structure (IS), considering that the displacement transducers are mounted on the latter.

NUMERICAL MODEL AND INSTRUMENTATION

The CS consists of a post-tensioned cylindrical shell capped by the spherical casket connected to the cylinder by a massive rectangular ring beam (Figure 1, left). The cylindrical section, with a thickness of 1.10 m, is stiffened by four vertical buttresses, each 1.90 m thick, that connect the base slab foundation to the upper ring beam. This post-tensioned base slab, 1.70 m thick, also supports the reinforced concrete IS. The spherical roof has a uniform wall thickness of 0.65 m.

A linear elastic finite element model (FEM) of the CS was developed using ABAQUS (2010) to evaluate the structural response to pressure leak-rate tests. The model comprises approximately 240,000 eight-node solid elements and 300,000 nodes. The flexibility of the foundation soil is represented by uniformly distributed horizontal and vertical springs, simulating the static behavior of the CS. The cylindrical shell was modeled with five elements across its thickness, while the ring beam and buttresses were modeled with nine, and the dome and base slab with four. The IS, also supported on the base slab, was represented using a coarse mesh to qualitatively assess the influence of the base slab's flexibility on experimental measurements.

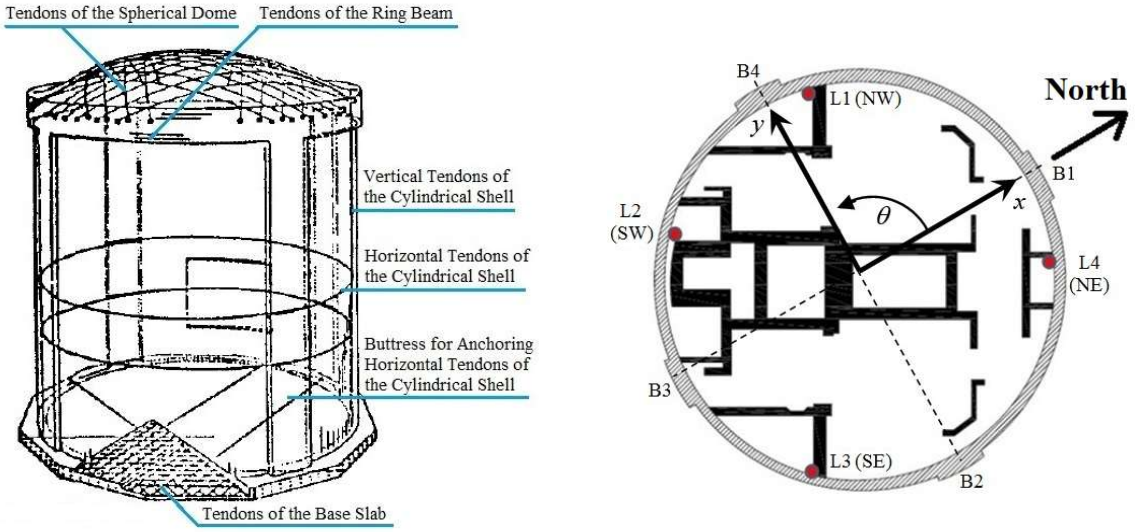

Figure 1. General layout of the CS of the Embalse NPP (left) and transducer location lines inside CS (right).

The FEM can simulate both the response to internal pressures and transient thermal changes across different sectors of the structure. The thermal input is defined based on measured temperatures from both the external and internal surfaces. Displacement and temperature measurements began one to two weeks before the pressurization process. Outer surface temperatures were recorded using thermographic cameras, while contact thermometers were placed along the internal surface. Displacements were recorded by means of 18 LVDTs that were fixed to both the CS and the IS, whereas the vertical displacement of the spherical dome was measured at the apex. Figure 1 (right) shows the position of lines L1, L2, L3 and L4 on which these transducers were located, while Table 1 shows their elevation.

The evolution over time of the relative atmospheric pressure inside the CS with respect to the atmospheric pressure outside for both analyzed tests is shown in Figure 2. This pressure first reached a value of 6 psi (41.4 kPa), remained constant for a period of time, after which the pressure increased to a peak value of 18 psi (124.1 kPa). A depressurization stage and a zero-pressure stage were then carried out, the latter in order to estimate possible permanent displacements in the structure.

Table 1. Designation and location of displacement transducers on the Containment Structure.

Dome		Line L1		Line L2		Line L3		Line L4	
Disp. trans.	Elev. [m]	Disp. trans.	Elev. [m]	Disp. trans.	Elev. [m]	Disp. trans.	Elev. [m]	Disp. trans.	Elev. [m]
MD01	145.1	MD11	100.0	MD21	98.2	MD31	100.0	MD41	101.8
		MD12	106.7	MD22	105.4	MD32	106.7	MD42	108.3
		MD13	112.5	MD23	112.5	MD33	112.5	MD43	113.9
		MD14	117.4	MD24	120.5	MD34	117.4	MD44	119.9
				MD25	128.1			MD45	128.8

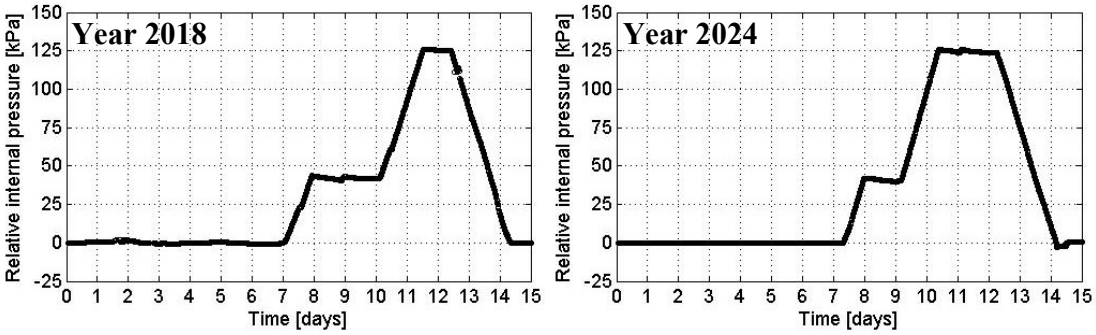

Figure 2. Evolution of internal pressure during the leak-rate test in 2018 (left) and 2024 (right).

INFLUENCE OF THERMAL CHANGES

In order to evaluate the influence of initial thermal conditions, Figure 3 presents a comparison of the temperature distribution across the thickness at point MD24 on the wall (1.10 m thick) and point MD01 near the center of the dome (0.65 m thick). The results indicate that by day 5.50, the temperature distributions across the thickness are largely independent of the initial temperature assumed for the internal nodes, while by day 10.50, the differences become imperceptible. It can be seen that the temperature distribution at day 0.50, starting on the same instant, initially exhibits a linear variation. However, for subsequent days, the computed temperature variation across the thickness deviates significantly from linearity and remains independent of the initial conditions assumed for the internal nodes. As a result, the temperature distribution obtained at day 7 (one week) is adopted as the initial condition for all nodes. This approach ensures that displacement calculations are based solely on the measured temperatures of the internal and external surfaces of the CS during the period when internal pressure is applied.

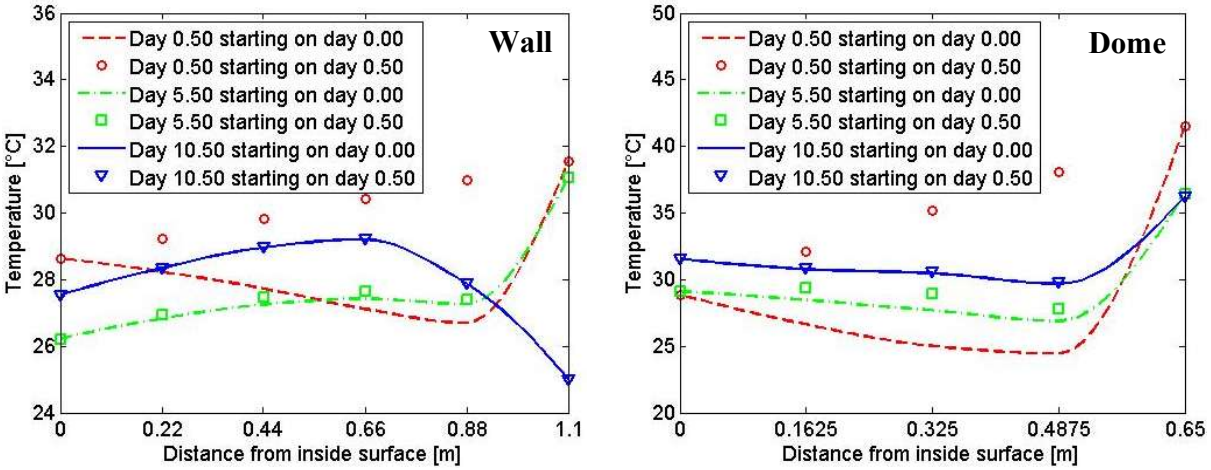

Figure 3. Evolution in time of the temperature distribution across the thickness at point MD24 on the wall (left) and at point MD01 near the dome apex (right) obtained from the numerical simulation.

Figure 4 presents a comparison of the temperature variation on the external surface of the CS between both tests. The 2018 test was conducted in the austral summer, while the 2024 test took place between the end of winter and the beginning of spring. Contrary to what might be expected, no significant variations are observed on the external concrete surface, except for the final days on the southern face. This could be attributed to the fact that during the summer, the sun shifts more toward the south at both the beginning and end of each day.

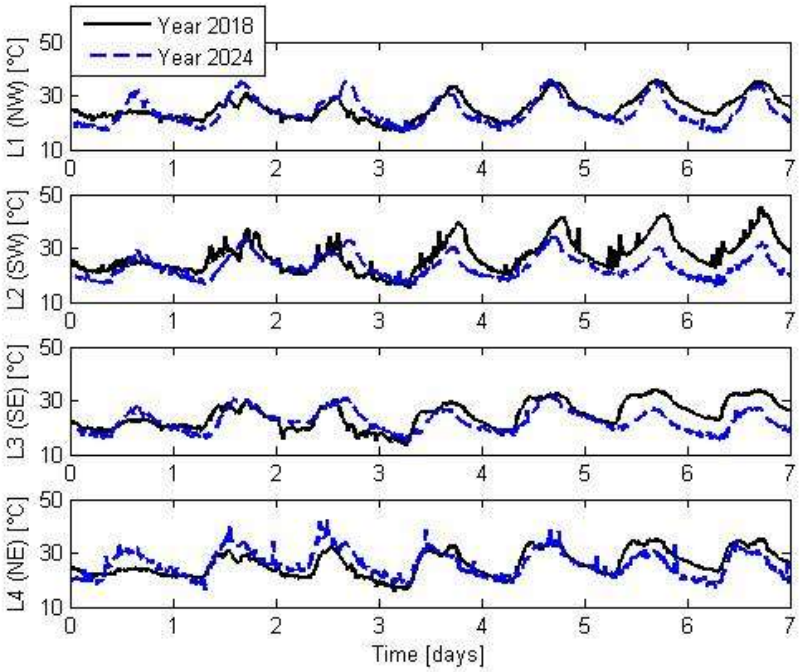

Figure 4. Temperature variation on the outer surface of the EC one week before the end of pressurization.

Figure 5 shows the total displacements caused by both internal pressure and temperature variations along line L2, which exhibits the highest values. As a reference, the displacements due only to pressure effects are also included. On the left, the displacements corresponding to the 2018 test are shown, while those for the 2024 test are presented on the right. At higher points, the measured and calculated displacements exhibit oscillations due to daily temperature changes exceeding 0.5 mm. These variations are of the same order of magnitude as the displacements for the first pressure step. The numerical model results, which take thermal changes into account, are not identical but are very close to the measured displacements. Therefore, the numerical model is considered representative of the observed behavior and can be used to filter out displacement components due to thermal changes, thereby isolating the displacements caused solely by pressure.

Figure 6 shows the filtered displacements obtained by following the reasoning from the previous paragraph. On the left, the values corresponding to the 2018 test are presented, where the measured displacements for the maximum pressure are slightly higher than the calculated ones, except for the lowest point, which has the smallest value. On the right side of the figure, the values for the 2024 test are displayed, where the trend remains the same, although with consistently larger differences. These differences can be partially attributed to the rigid body rotation of the internal structure supporting the displacement transducers, due to a particular deformation of the base slab, which is described later in this paper.

The maximum, average, and minimum displacements due solely to temperature are shown in Figures 7 and 8 for the 2018 and 2024 tests, respectively. These displacements correspond to a one-week period covering both pressure steps and ending at the moment depressurization begins. The need for thermal correction is evident in these figures, where the absolute value of the displacements exceeds 0.5 mm at several points, while the peak-to-peak variation for line L2 in the 2018 test exceeds 1 mm at the highest points.

The maximum displacements caused by pressure for both tests are presented in Figure 9, where it can be seen that the displacements corresponding to line L2 match those indicated in Figure 6 at maximum pressure. The calculated displacements for lines L1 and L3 show little difference from the measured values in both tests. On the other hand, for line L2, the measured displacements are greater than the calculated ones, while for line L4, the opposite occurs. As observed in Figure 1 (right), lines L1 and L3 are located on either side of the internal structure's symmetry plane, whereas lines L2 and L4 lie on the symmetry plane. Thus, lines L1 and L3 are not significantly affected by an axially symmetric deformation of the base slab, since the structure responds symmetrically and does not generate radial displacements perpendicular to the symmetry plane. Conversely, lines L2 and L4 are affected, as the internal structure can deform almost like a rigid body within the symmetry plane, causing displacements of the transducer attachment points in the radial direction. This increases relative displacements in one line (L2) while decreasing them in the other (L4). This behavior is precisely observed in the reported results.

Figure 10 illustrates the deformation of the base slab evaluated by means of a numerical model, in the symmetry plane of the internal structure. Line L4 is located on the left side, where the internal structure moves closer to the containment structure, leading to smaller relative displacements. On the other hand, line L2 is on the right side, where larger relative displacements occur due to the increasing separation between the two structures.

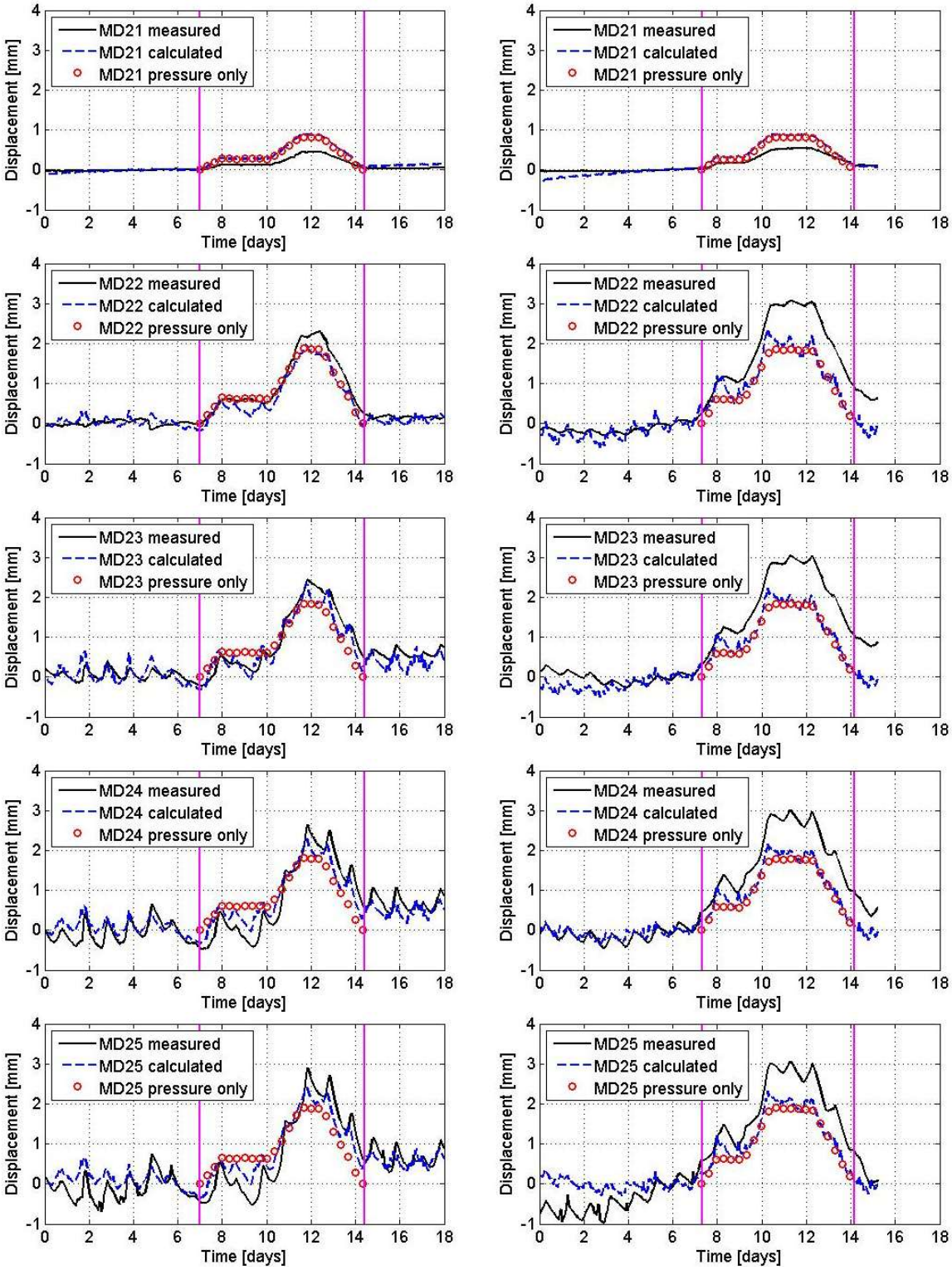

Figure 5. Total displacements due to pressure and temperature in 2018 (left) and 2024 (right).

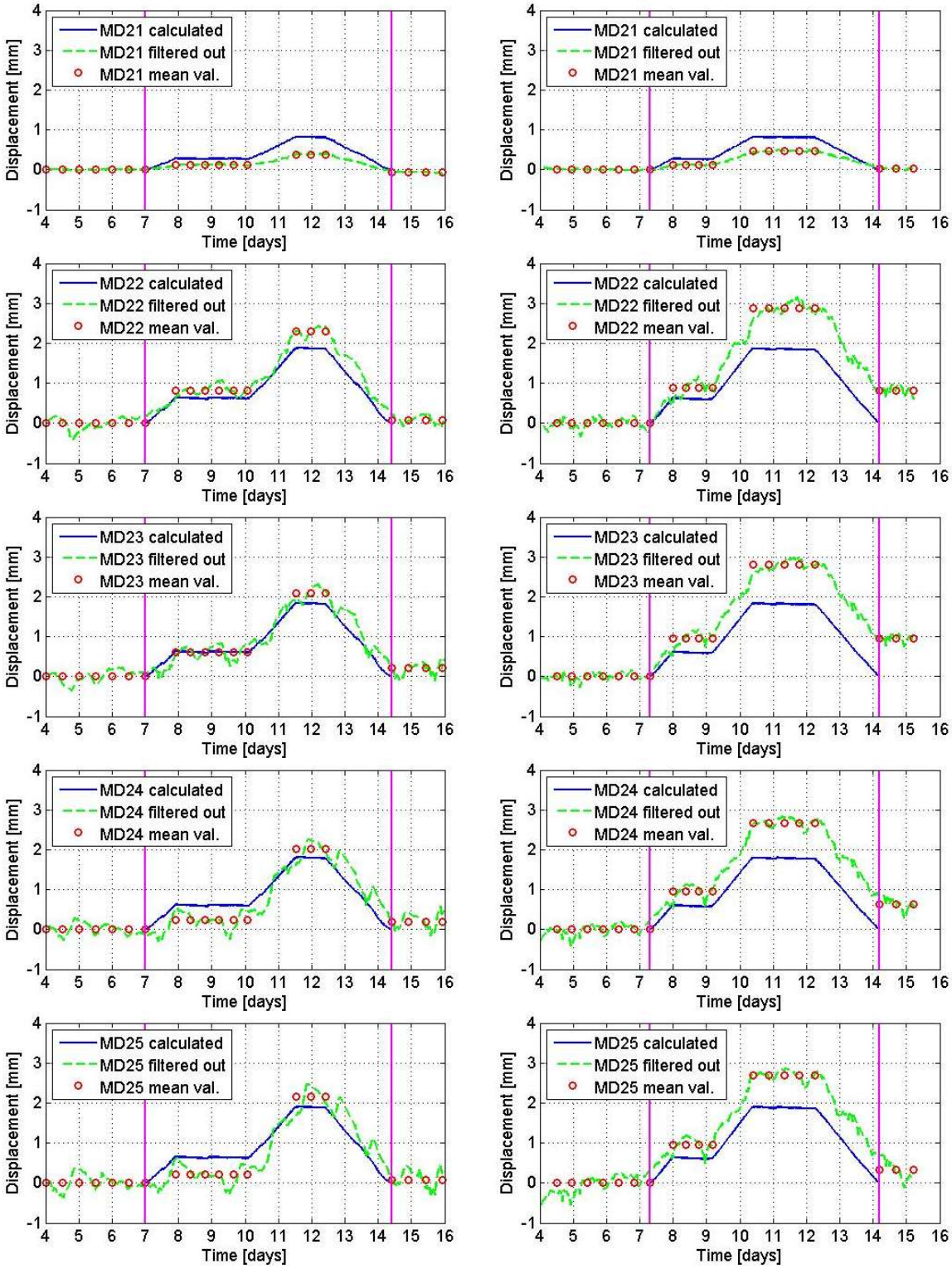

Figure 6. Displacements due only to pressure in 2018 (left) and 2024 (right).

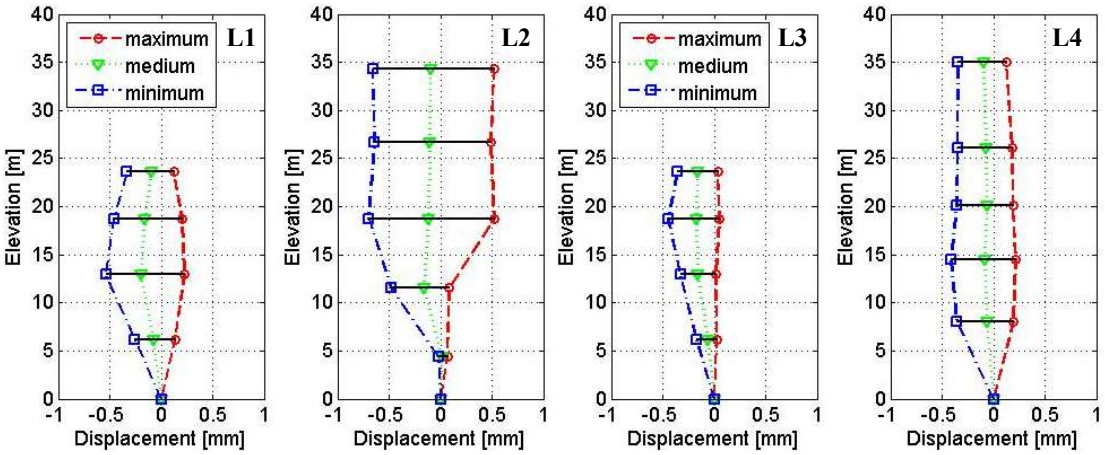

Figure 7. Displacements caused by a week of thermal variation in 2018 test on lines L1 to L4.

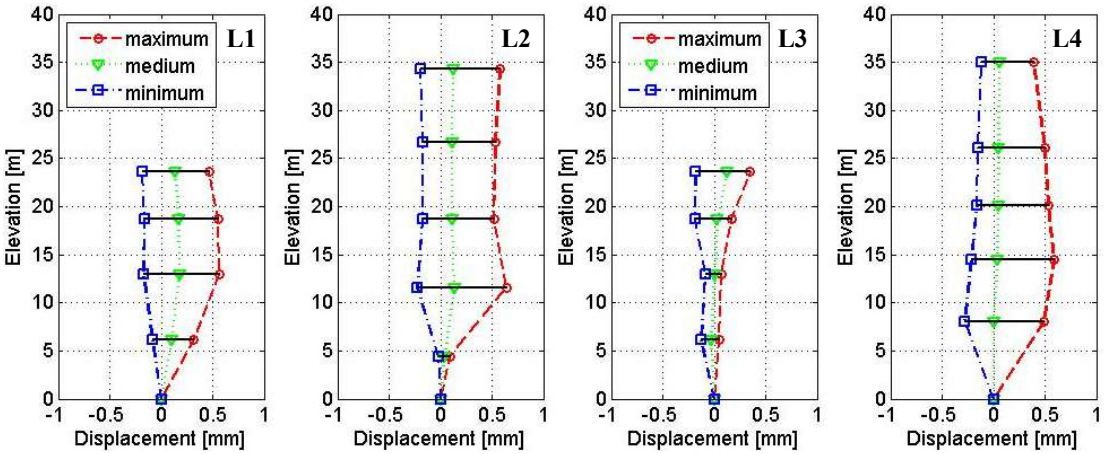

Figure 8. Displacements caused by a week of thermal variation in 2024 test on lines L1 to L4.

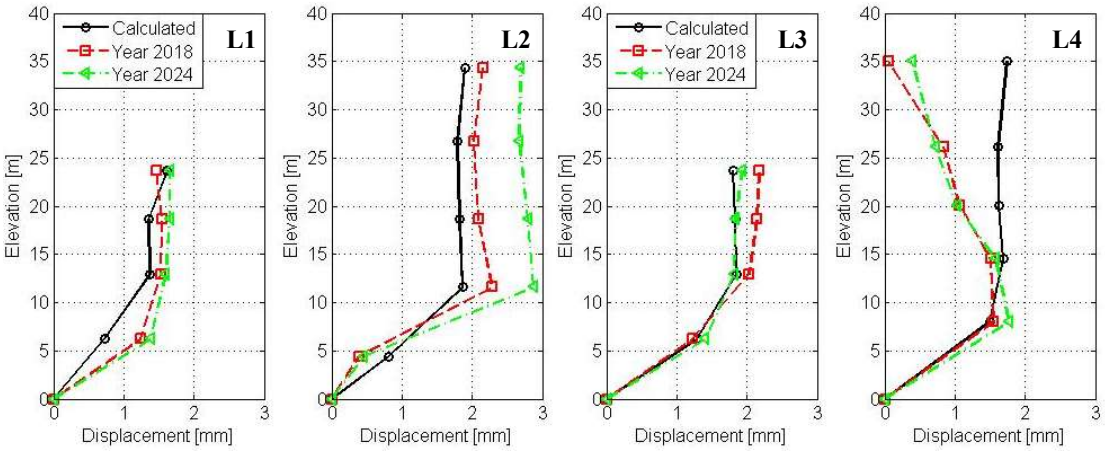

Figure 9. Maximum displacements caused by internal pressure on lines L1 to L4.

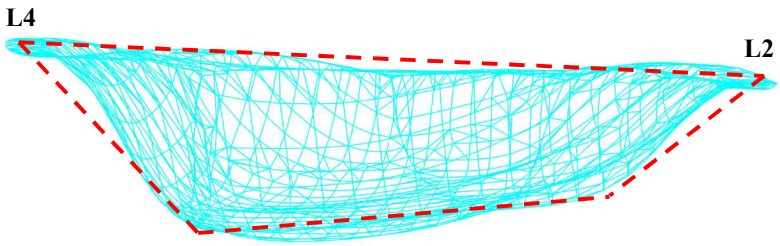

Figure 10. Base slab deformation during a pressure test.

To reduce the influence of rigid body rotation caused by deformations on the base slab on the measurements, the relative displacements between diametrically opposed lines were calculated. Figure 11 presents both the displacements between lines L1 and L3 (left) and those between lines L2 and L4 (right). In the latter case, this compensatory approach significantly reduces the discrepancies observed between the calculated and measured values, highlighting the influence of base slab deformations on the relative displacement between the two structural components.

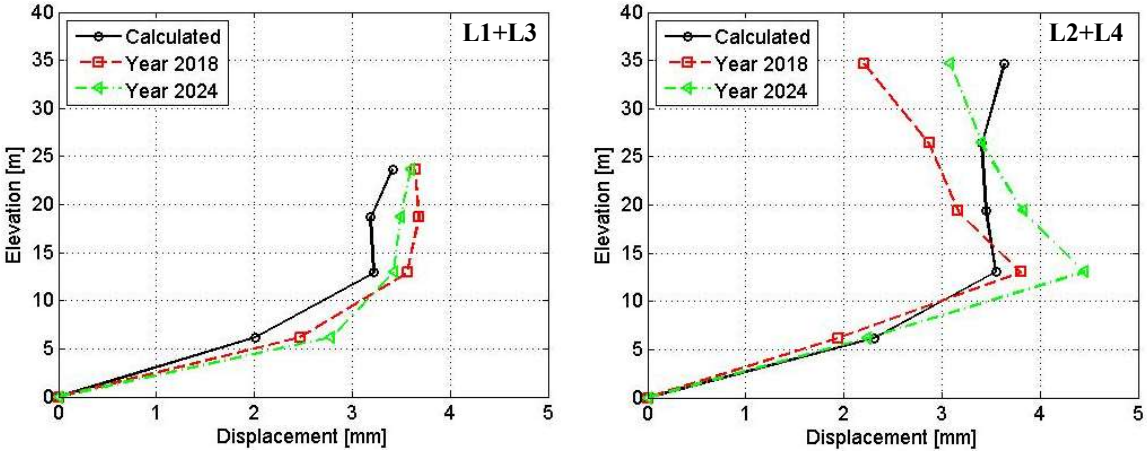

Figure 11. Relative displacements between lines L1 and L3 (left), and between lines L2 and L4 (right).

CONCLUSIONS

Thermal variations during leakage rate tests of nuclear containment structures can cause significant displacement oscillations, potentially obscuring the structure's response to applied pressures. This effect is particularly relevant across different seasons. Therefore, detailed temperature monitoring both inside and outside the structure is essential for accurately interpreting the results, using a numerical model capable of accounting for transient thermal effects.

It is also important to account for base slab deformation, particularly if displacements are measured with respect to the internal structure, as these reference points may undergo significant displacements during the pressurization stages.

REFERENCES

ABAQUS Finite Element Software v6.10 (2010). *Dassault Systèmes Simulia Corp.*, Providence, RI, USA.

Ceballos, M.A., Estrada, C.F., Pinto, F., Pomerantz, M. and Prato, C.A. (2019). "Structural evaluation of a reactor building during pressure testing for life extension assessment", *5th Int. Conference on Smart Monitoring, Assessment and Rehabilitation of Civil Structures (SMAR 2019)*, Potsdam, Germany.

Cheng, S., Kwon, O-S., Bentz, E. and Tcherner, J. (2022). "Comparison of measured strain and thermal effects during reactor building leakage rate tests of a nuclear power plant", *Engineering Structures*, Vol. 271, 114898.

Kim, H-C., Pak, S-K., Lee, J-S., Cho, S-W. (2018). "Validation of the MELCOR input model for a CANDU PHWR containment analysis by benchmarking against integrated leakage rate tests", *Nuclear Engineering and Design*, Vol. 340, pp. 201–218.

Pinto, F., Ceballos, M.A., Estrada, C.F., Barrera, A. and Prato, C.A. (2024). "Evaluation of the Structural Response of the Containment Structure of a NPP to Internal Pressure and Thermal Gradients", *7th International Conference on Smart Monitoring, Assessment and Rehabilitation of Civil Structures (SMAR 2024)*, Salerno, Italy.

Wang, X., Huang, X., Kwon, O-S., Bentz, E., Tcherner, J., DeMerchant, M., Moland, M. (2019). "Evaluation of the thermal strain of an NPP containment structure during leakage rate tests", *Engineering Structures*, Vol. 201, 109761.